Accelerated Publications

The Structure of Photosystem II in *Arabidopsis:* Localization of the CP26 and CP29 Antenna Complexes†

Alevtyna E. Yakushevska,‡ Wilko Keegstra,‡ Egbert J. Boekema,‡ Jan P. Dekker,§ Jenny Andersson,|| Stefan Jansson,|| Alexander V. Ruban,⊥ and Peter Horton*,⊥

Biophysical Chemistry, Groningen Biomolecular Sciences and Biotechnology Institute, University of Groningen, Nijenborgh 4, 9747 AG Groningen, The Netherlands, Faculty of Sciences, Division of Physics and Astronomy, Vrije Universiteit, De Boelelaan 1081, 1081 HV Amsterdam, The Netherlands, Umeå Plant Science Centre, Department of Plant Physiology, Umeå University, S-901 87 Umeå, Sweden, and Robert Hill Institute, Department of Molecular Biology and Biotechnology, University of Sheffield, Firth Court, Western Bank, United Kingdom

Received November 4, 2002; Revised Manuscript Received December 2, 2002

ABSTRACT: A genetic approach has been adopted to investigate the organization of the light-harvesting proteins in the photosystem II (PSII) complex in plants. PSII membrane fragments were prepared from wild-type *Arabidopis thaliana* and plants expressing antisense constructs to *Lhcb4* and *Lhcb5* genes, lacking CP29 and CP26, respectively (Andersson et al. (2001) *Plant Cell 13,* 1193−1204). Ordered PS II arrays and PS II supercomplexes were isolated from the membranes of plants lacking CP26 but could not be prepared from those lacking CP29. Membranes and supercomplexes lacking CP26 were less stable than those prepared from the wild type. Transmission electron microscopy aided by single-particle image analysis was applied to the ordered arrays and the isolated PSII complexes. The difference between the images obtained from wild type and antisense plants showed the location of CP26 to be near CP43 and one of the light-harvesting complex trimers. Therefore, the location of the CP26 within PSII was directly established for the first time, and the location of the CP29 complex was determined by elimination. Alterations in the packing of the PSII complexes in the thylakoid membrane also resulted from the absence of CP26. The minor light-harvesting complexes each have a unique location and important roles in the stabilization of the oligomeric PSII structure.

Photosystem II (PSII)[1] is the multisubunit thylakoid membrane associated complex, consisting of over 25 subunits (*1*), that uses energy of sunlight to drive the oxidation of water, evolving oxygen, donating electrons into the photosynthetic electron transfer chain, and depositing protons into the thylakoid lumen. An important aspect of PSII function relates to the design, assembly, and regulation of the light-harvesting complexes (LHC), which form the major part of the PSII antenna (*2*). The PSII antenna functions to increase the rate of excitation energy delivery to the PSII by at least 2 orders of magnitude, ensuring a sufficient rate of the light energy input into photosynthesis. The LHC antenna of PSII is complex and heterogeneous, consisting of six different proteins named Lhcb1−6 (*3*), encoded by a large multigene family (*4*). Lhcb4, Lhcb5, and Lhcb6 form the monomeric complexes CP29, CP26, and CP24, respectively, and Lhcb1, Lhcb2, and Lhcb3 associate in different combinations into trimers of the main complex, LHCII, that binds 60% of all the chlorophyll in PSII (*5*). The conservation of *Lhcb* genes for nearly 350 millions years in all angiosperms and gymnosperms argues strongly in favor of a specific role for each one in PSII (*4*).

Despite extensive biochemical and spectroscopical studies, the specific functions of the Lhcb proteins remain poorly understood. In particular, the functions of the monomeric CP26 and CP29 complexes are unknown, although many have been suggested. Interestingly, although they are not required for photosynthesis per se, they are necessary for maximum quantum efficiency (*6*). Central to resolving this uncertainty is to determine their structural topography within the PSII complex, and to thereby understand their role in the molecular design and function of PSII. To date, all

† Supported by the UK Biotechnology and Biological Sciences Research Council Grant 50/C11581, the UK Joint Infrastructure Fund, The Netherlands Foundation for Scientific Research (NWO) via the Foundation for Life and Earth Sciences (ALW) and the Swedish Research Council for Environment, Agricultural Sciences and Spatial Planning and the Foundation for Strategic Research.

* Corresponding author. Address: Department of Molecular Biology and Biotechnology, University of Sheffield, Firth Court, Western Bank, Sheffield S10 2TN, U.K. Tel: +44 114 222 4189. Fax: +44 114 222 2787. E-mail: p.horton@sheffield.ac.uk.

‡ University of Groningen.

§ Vrije Universiteit.

|| Umeå University.

⊥ University of Sheffield.

[1] Abbreviations: PSII, Photosystem II; LHCII, the major light-harvesting complex of photosystem II; CP26 and CP29, the minor PSII antenna complexes; C_2S_2, the PSII supercomplex containing a dimeric PSII core and two strongly bound trimeric LHCII complexes; M_2, two moderately bound LHCII trimers.

10.1021/bi027109z CCC: $25.00
Published on Web 12/28/2002

structural models (e.g., refs *7*, *8*) showing the locations of CP29 and CP26 are based upon indirect evidence. Structural studies on PSII−LHCII associates (LHCII−PSII supercomplexes) using single particle analysis of EM images of both solubilized PSII membranes (*9*−*11*) and ordered arrays of PSII complexes in membrane fragments (*12*, *13*) have revealed that there are areas of density with the estimated size of a monomeric LHC complex. Biochemical analysis of a purified supercomplex preparation (*14*) showed the presence of CP26 and CP29, and it was therefore assumed that two areas, on either side of the supercomplex, are occupied by these two proteins. Since CP26 and CP29 are predicted to have a similar overall shape, it obviously could not be deduced at which of the two potential sites CP26 and CP29 were located. The assignment of CP26 and CP29 in the complex is therefore based only on the study of cross-linking products (*15*). These studies suggested that CP26 was close to CP43 and that CP29 was close to D2, but the possibility of close proximity between CP29 and CP43 could not be excluded. Moreover, the recent X-ray model of PSII (*16*) clearly pointed to an alternative position of the D2 protein to that assumed in (*15*), which also complicates any tentative assignments based on this work.

A direct approach to assign unambiguously the location of the CP26 and CP29 complexes would be to use plants lacking each of these proteins and to compare them with the wild-type plants. We have therefore used reverse genetics and created *Arabidopsis* plants deficient in specific LHC proteins by the expression of antisense (as) genes. Expression of *asLhcb4* and *asLhcb5* genes led to plants, which have no CP29 and no CP26, respectively (*6*). Here we use these plants to directly assign the position of the CP26 subunit by electron microscopy analysis of ordered PSII arrays and of isolated PSII−LHCII supercomplexes obtained from *asLhcb5* plants. Our data show the CP26 position clearly to be at the tips of the supercomplex. Supercomplexes were also found to be less stable in *asLhcb5* plants and completely absent from the *asLhb4* plants lacking CP29, implying an important role of the minor antenna complexes in the stability and assembly of the PSII supercomplex. Further, it was found that CP26 also influences the supramolecular organization of the complexes in the thylakoid membrane.

MATERIALS AND METHODS

Plant Materials. *Arabidopsis thaliana* cv Columbia plants were grown in growth chambers at 8 h photoperiod and 200 μmol quanta m^{-2} s^{-1} for 8 weeks as previously described (*17*). The *asLhcb4* and *asLhcb5* lines show complete absence of Lhcb4 and Lhcb5 gene products, respectively, but unchanged levels of other Lhcb proteins, except for some depletion of CP24 in *asLhcb4* (*6*).

Preparation and Fractionation of PSII Membranes. PSII membranes were prepared according to the protocol originally developed for spinach (*18*), but with some modifications. In brief, leaves were harvested and mixed with the chilled grinding buffer (20 mM Tricine-NaOH, pH 8.4, 0.45 M sorbitol, 10 mM EDTA, 0.1% BSA) and homogenized three times for 5 s. After pelleting and washing in wash buffer (0.3 M sorbitol, 20 mM Tricine NaOH, pH 7.6, 5 mM $MgCl_2$), chloroplasts were osmotically shocked for 30 s. Pelleted thylakoids were incubated in the stacking medium for 1 h, after which they were treated with 2.5% Triton X-100 at 3 mg chl/mL concentration. After 30 min of incubation, the PSII membranes were sedimented at 30 000*g* for 30 min and resuspended in a buffer containing 20 mM Bis-Tris (pH 6.5) and 5 mM $MgCl_2$. Membrane fragments and PSII supercomplexes were obtained after solubilization of the PSII membranes with 0.4% *n*-dodecyl-α-D-maltoside (α-DM) at a Chl concentration of 1.4 mg/mL. Large fragments were removed by centrifugation for 3 min at 9000 rpm in an Eppendorf tabletop minifuge and the supernatant was promptly filtered through a 0.45 mm filter. Finally the sample was subjected to gel-filtration chromatography, using a Superdex 200 HR 10/30 column in an Amersham-Pharmacia Åcta Purifier system using the same buffer and similar conditions as described in (*19*). Isoelectric focusing of *n*-dodecyl-*β*-D-maltoside (*β*-DM) solubilized PSII membranes was carried out as described by Ruban et al. (*20*). Separation of solubilized PSII membranes on a sucrose gradient was performed using the method described in (*21*). Room-temperature absorption spectra of samples were recorded in the 1 cm cuvette at chlorophyll concentration of 4 g/mL using a Varian Cary 50 spectrophotometer.

Electron Microscopy and Image Analysis. The two first fractions after gel filtration eluting around 17 and 19 min were immediately after chromatography prepared for electron microscopy, using 2% uranyl acetate as negative stain. Membrane fragments and supercomplexes were analyzed in a similar way as was previously done using preparations from spinach and the wild type *Arabidopsis* plants (*10*, *12*, *13*). The samples were imaged in a Philips CM10 electron microscope at 52 000× magnification. Electron micrographs were digitized with a Kodak Eikonix Model 1412 CCD camera. Single particle projections were extracted from negatives and analyzed with IMAGIC software and Groningen Image Processing ("GRIP") software. Single particle projections were obtained by selecting all discernible particles from 75 negatives. From 107 digitized negatives of paired inside-out membranes with crystalline arrays from the *asLhcb5* plants, we selected 3088 partially overlapping fragments with a size of 144 × 144 pixels (or 700 × 700 nm). The averaged projection of the wild-type crystal (taken from (*13*) was used as a first reference. Subsequently, the aligned fragments were submitted to multivariate statistical analysis and classification (*22*, *23*). For the second alignment run, we used the best class-sum as a next reference. This reference led to a further improvement of the accuracy of alignment and classification. From the last classification, 876 fragments from the best classes were summed. In the case of wild-type paired membrane crystals, this procedure turned out to be sufficient to filter out the contribution of the second crystal layer. However, in the case of the *asLhcb5* plants, the contribution of the second layer was still visible after summation. To remove the second layer contribution, the image was Fourier transformed, and the two superimposed crystalline lattices were separated (see ref *13* for a similar example). The back-transformed image contained the projected density of only a single layer

RESULTS AND DISCUSSION

Gel-Filtration Analysis of PSII Membranes. The strategy used for structural analysis was the same as developed recently (*12*, *13*, *19*) and involves very mild detergent treatment of PSII membranes, followed by rapid fractionation

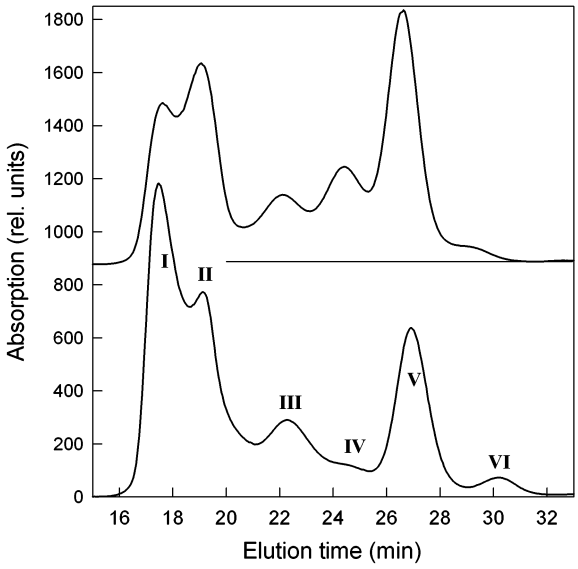

FIGURE 1: Gel filtration elution profiles of *n*-dodecyl-α-D-maltoside solubilized photosystem II membranes from wild type (bottom) and *asLhcb5* (top) samples, detected at 670 nm. The main fractions are designated I−VI. From previous work (*19*) it is known that these fractions contain the following: I, membrane fragments; II, PSII−LHCII supercomplexes; III, PSI; IV, PSII cores; V, LHCII trimers; VI, monomeric light-harvesting complexes.

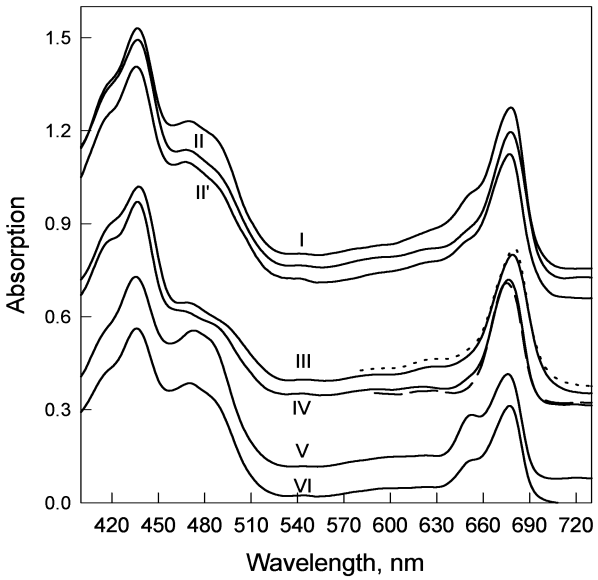

FIGURE 2: Room-temperature absorption spectra of the six main gel-filtration fractions from the wild-type sample (see Figure 1). I, membrane fragments; II, PSII−LHCII supercomplexes; II′, PSII−LHCII supercomplexes from *asLhcb5* plants; III, PSI; IV, PSII cores; V, LHCII trimers; VI, monomeric light-harvesting complexes. Dashed and dotted lines are respectively the red-region absorption spectra of a PSII core preparation and PSI isolated from the solubilized PSII membranes from spinach by sucrose gradient centrifugation (*20*).

by gel filtration. The samples are then immediately prepared for EM analysis. Although this rapid separation procedure does not yield highly purified samples, for EM analysis this is not critical because the applied image analysis procedures allow the projections of single PSII molecules plus eventual contaminants to be classified. Moreover, the major advantage of this procedure is that membrane fragments containing ordered arrays of PSII membranes can also be obtained in the same gel-filtration. This allows an analysis of the supercomplex structure and the macro-organization of the complexes in the thylakoid membrane to be obtained. Figure 1 shows the gel-filtration chromatograms of mildly solubilized PSII membranes obtained from wild type and *asLhcb5* plants, recorded at 670 nm to monitor chlorophyll content. The elution profile of the wild type plant (Figure 1, bottom line) shows a strong similarity to that obtained previously (*19*), and the compositions of these fractions were confirmed by observation of their absorption spectra. The first main fractions (I and II) were attributed to the PSII grana membrane fragments and PSII−LHCII supercomplexes, respectively. As expected, the absorption spectra of the Fractions I and II are very similar to those shown previously (*19*) (Figure 2, traces I and II). Similarly, Fraction III is assigned to monomeric PSI-200 complexes, the absorption spectrum being almost identical to that of a purified PSI fraction (Figure 2, trace III and the overlapping dotted curve). The minor Fraction IV arises from PSII core monomers, and again the absorption spectrum is similar to that of a purified monomeric PSII fraction (Figure 2, trace IV and dashed curve). Fractions V and VI originate from the major, trimeric LHCII and from monomeric LHC complexes, respectively. The absorption spectrum of the Fraction V resembles closely that of purified LHCII (*21*).

The chromatograms from the *asLhcb5* plants gave different elution profiles (Figure 1, top curve). There was a decrease in the amount of chlorophyll in Fractions I and II. On the other hand, the LHCII trimer Fraction V was much stronger in the antisense line, and Fraction IV, the monomeric PSII core complex, was also much more apparent. Together these data indicate a decrease in stability of the PSII−LHCII supercomplex in the antisense plants, with correspondingly a larger fraction of PSII monomers and LHCII trimers. The absorption spectrum of the supercomplex from the *asLhcb5* plants was almost identical to that of the wild type (Figure 2, trace II′).

The chromatogram for the antisense plants lacking CP29 (*asLhcb4*) was similar to that of *asLhbc5* (not shown). However, in this case Fraction II was greatly decreased, indicating a dramatic reduction in the fraction of PSII−LHCII supercomplexes. We tested different strategies for solubilization of the thylakoid membrane, such as the use α-DM instead of Triton X-100 to prepare PSII membranes (*19*) and the use of lower α-DM concentrations to disrupt the membranes. However, we were never able to recover significant chlorophyll in Fraction II. These experiments indicated that the membranes from the *asLhcb4* plants are much less resistant to detergents than wild-type membranes so that the PSII−LHCII supercomplexes are less stable and possibly even absent.

Localization of CP26 in Isolated PSII−LHCII Supercomplexes. To investigate the structure of the supercomplexes from the *asLhcb5* plant, EM was used to analyze Fraction II, where PSII−LHCII supercomplexes were expected. From 75 negatives, only about 180 potential PSII−LHCII particle projections could be selected. Multireference alignment, multivariate statistical analysis and classification revealed only one class of PSII projections, shown in Figure 3A. This class resembles the "standard" C_2S_2 PSII−LHCII supercomplex found in wild type plants (Figure 3C) (*11*). However, it misses tips on two of its corners. A similar type of

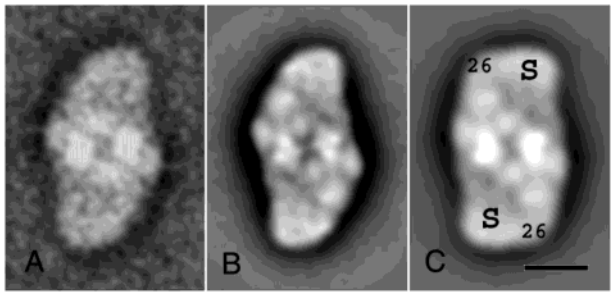

FIGURE 3: Single-particle image analysis of PSII−LHCII supercomplex projections, from material obtained in Fraction II. (A) Averaged image of the 15 projections from *asLhcb5* plants lacking CP26; (B) for comparison, averaged image of 300 projections obtained by classifying large heterogeneous data sets of supercomplexes in spinach; (C) averaged image of 218 projections from wild type *Arabidopsis*. The image denotes the C_2S_2 supercomplex that contains just two S-type LHCII trimers per core dimer and which has space for two monomeric antenna complexes. The image shows the identified location of CP26, and by inference, CP29. The bar is 10 nm.

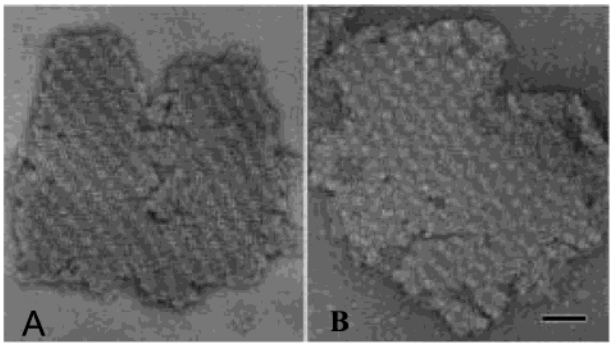

FIGURE 4: Electron micrographs of negatively stained paired grana membrane fragments obtained from Fraction 1, *asLhcb5* (A), and wild-type (B) *Arabidopsis* showing the crystalline arrays of PSII−LHCII supercomplexes. The space bar is 50 nm.

projection has been found previously with low frequency by classifying large heterogeneous data sets in spinach (Figure 3B), and it was suggested to result from the loss of a minor antenna complex (*7*). The missing tips in the single particle sum obtained from the antisense plants show directly that CP26 is located in these areas.

The Localization of CP26 in PSII Ordered Arrays. To support the conclusion obtained from analysis of the population of isolated supercomplexes, we examined Fraction I with EM to test for the presence of paired grana membrane fragments containing ordered arrays of PSII−LHCII supercomplexes. As found previously for wild-type *Arabidopsis* membranes (*13*), about 10% of the fragments showed macrodomains with an ordered crystalline lattice of rows of PSII complexes on both membranes of the granum (Figure 4). Such arrays are not perfectly ordered but still suitable for structural analysis at low to medium resolution.

The results of image analysis are shown in Figure 5. There were significant differences between the wild type and antisense images. The crystal from the *asLhcb5* plant has unit cell dimensions of 25.7 × 19.5 nm, an angle of 86° between the axes, and a unit cell area of 500 nm^2 (Figure 5A). In contrast, the unit cell from the wild-type membranes has dimensions of 25.7 × 21.4 nm, an angle of 77°, and an area of 534 nm^2 (Figure 5B). Hence, the vertical spacing between the cores (bright features) was different, decreasing from 21.4 nm in the wild type to 19.5 nm in the antisense. In the horizontal direction, the distance of 25.7 nm between the cores remained the same. There was also a difference in the orientation of the cores in the lattice. Most importantly, there are clearly differences seen at the tips of the core: the spacing between the tips of adjacent cores is smaller; the densities around the tips are different; and the tips juxtapose with a different orientation.

It should be pointed out that because negative stain tends to accumulate more at the base of a protein and into cavities, the true protein density is not exactly observed. Although PSII is a rather flat structure, it has a strongly protruding oxygen-evolving complex, around which stain accumulates, tending to obscure the areas where the minor antenna complexes are found. At the resolution of these images, which is close to 3 nm for the arrays from antisense plants and 2 nm for the wild type, the trimers are just visible. There is little detail of their internal features, and the exact borders of minor antenna proteins cannot be determined. However, the features of the core in both samples are very well defined, and this allows a fitting of a PSII−LHCII supercomplex obtained from single particle analysis as previously performed (*13*). For this, we used the $C_2S_2M_2$ type of supercomplex that was previously shown to be the predominant form in wild type *Arabidopsis* membranes (*13*). This complex contains the dimeric core (C), spaces for six monomeric complexes (green areas), and four LHCII trimers (yellow areas, S and M). For the wild type, all these features can be fitted to the image of the PSII array (ref 13 and Figure 5E). However, in the case of the *asLhcb5* plant, the complete supercomplex cannot be fitted: there is not enough space for two areas on the lower left and upper right tips (Figure 5D). These are exactly the same areas, which are missing from the isolated PSII supercomplex from the antisense plant (Figure 4). Therefore, we conclude, unequivocally, that each of these tips is the location of a CP26 complex. The alteration in the supercomplex structure also explains why the orientation and spacing of the lattice is changed: in the absence of CP26, the supercomplexes are packed closer together. Hence, not only does the removal of CP26 alter the supercomplex structure, it alters the way in which they are packed in the thylakoid membrane.

Electron Microscopical Analysis of asLhcb4 Plants. To gain insight into the organization of PSII prepared from the *asLhcb4* plant lacking CP29, we examined Fraction I from the gel-filtration chromatography by EM. The paired grana membranes, obtained after a 0.4% α-DM treatment of chloroplasts, were found to be partially solubilized because many stain-filled holes were visible. The size of the particles observed and their distribution resembled those of PSII core dimers in membranes from wild-type *Arabidopsis* (not shown), but there was no tendency to form two-dimensional arrays. Therefore, it was not possible to get further information about the presence of specific types of supercomplexes in the membrane. Moreover, examination of images made from Fraction II where purified PSII−LHCII supercomplexes were expected indicated that supercomplexes were totally absent. Nevertheless, by elimination, the assignment of the location of CP26 establishes the CP29 position (Figure 4D,E). The third minor antenna complex CP24 probably occupies the remaining space in the $C_2S_2M_2$ PSII−LHCII supercomplex, as shown by its absence from the C_2S_2

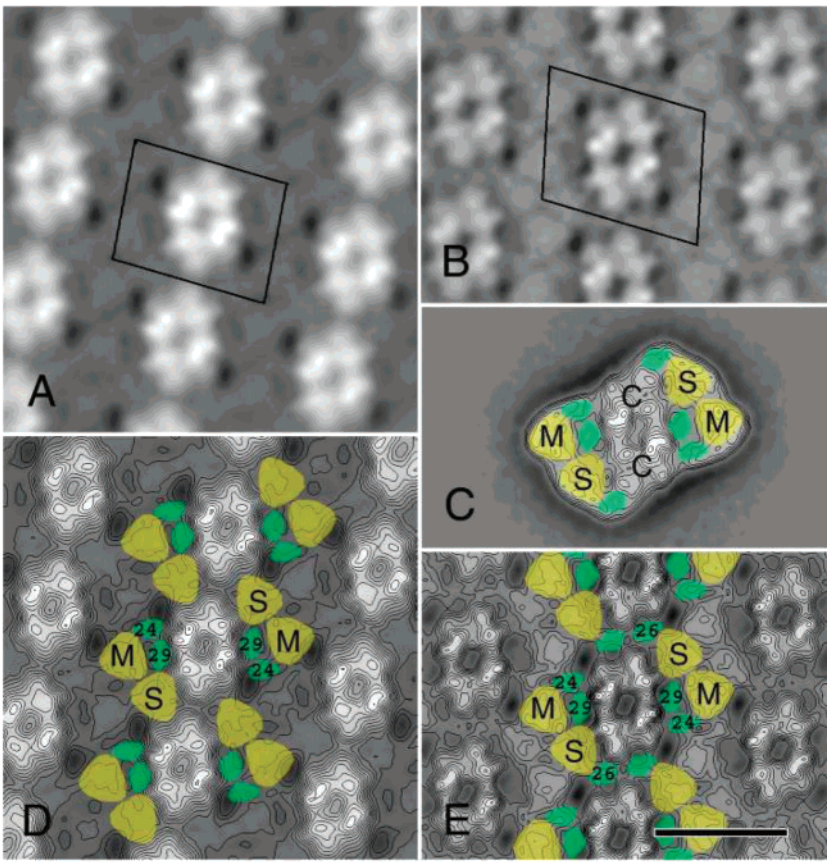

FIGURE 5: Image analysis of the ordered PSII arrays in membrane fragments. (A) The sum of 867 images from *asLhcb5* plants; (B) the sum of 450 images from wild-type plants (taken from ref *13*). The unit cells or repeating motifs of both crystals are indicated—there is a difference in size and angle between the axes (see text); (C) the averaged projection of an *Arabidopsis* $C_2S_2M_2$ supercomplex obtained from previous work (*13*), which is used to fitting, showing the position of the PSII cores (C), the S and M-types of LHCII trimers (yellow), and minor antennae complexes (green); (D) contour version of the *asLhcb5* image (A) with the position of the S-type and M-type LHCII trimers, and CP29 and CP24 indicated; (E) contour version of the image (B) with the position of the S-type and M-type LHCII trimers, and CP29, CP26, and CP24 indicated. Note the absence in D of the two areas at the tips of the supercomplex seen in panel A.

complex (*14*). Within the C_2S_2 PSII−LHCII supercomplex, CP29 is close to the CP47 subunit, and a cross-link with CP47 was found (*14*, *24*). This assignment also predicts that CP29 will be close to CP24 in the $C_2S_2M_2$ PSII−LHCII supercomplex, again in agreement with the cross-linking data (*25*). Furthermore, a close proximity of CP29 and CP24 is consistent with the fact that the *asLhcb4* plants missing CP29 are also deficient in CP24 (*6*).

CP26 and CP29 Are Important in Stability of the PSII−LHCII Supercomplex. It is evident from the EM and gel filtration experiments that the absence of the CP26 or CP29 subunits reduces the stability of the PSII−LHCII supercomplexes. For CP26, in its absence, PSII−LHCII supercomplexes can still be formed, although the supercomplexes are less stable and the grana membranes are more vulnerable to detergents. The deletion of the CP29 protein has a particularly detrimental effect because no supercomplexes could be detected by electron microscopy. In the absence of CP29, the strongly bound LHCII trimers (S-type trimers) appear to have been released (*11*). These results are consistent with previous indirect observations on spinach supercomplexes. Although some supercomplexes had been found after isolation that lacked what we have now proved to be the CP26 subunit, no native supercomplexes were ever detected without what we now assign to be CP29 (*7*, *10*). Furthermore, previous measurements made on thylakoids prepared from the antisense plants indicated that PSII is more labile in plants lacking CP29 (*6*).

The Function of CP29 and CP26. Previously it was shown that there were decreases in PSII quantum yield in the antisense plants lacking CP26 and CP29 (*6*). In the case of plants lacking CP29, this was associated with an increase in the F_o level of chlorophyll fluorescence, suggesting a decrease in the efficiency of trapping of excitation by the reaction center. In the absence of CP26, the lower PSII quantum yield was associated with a quenching of the F_m level of chlorophyll fluorescence. Quenching of F_m could arise from altered interactions between the LHCII on adjacent supercomplexes that result from the change in packing of the complexes in the thylakoid membrane. This implies that the minor antenna complexes play important roles in the assembly of PSII into the supercomplex and the macroorganization of supercomplexes in the thylakoid membrane. These structural features of PSII are required to maintain its high quantum efficiency. Consequently, from this notion we begin to understand the very precise design of the PSII. In this case, the function of the minor antenna is related to this vital structural role in PSII, and perhaps not to any other specific function. For example, CP26 is not required for energy transfer from LHCII to the PSII core, and neither complex appears to be required for the regulation of light harvesting (*6*). However, it is important to stress that our

results show that CP29 and CP26 each has a unique role and location in the oligomeric structure of PSII. The absence of either CP29 or CP26 does not lead to its replacement by another complex.

ACKNOWLEDGMENT

We are grateful to Mrs. Pamela Lee for her advice on preparing photosystem II particles from *Arabidopsis* and Dr. Mark Wentworth for helpful discussion and Mr. John Proctor for the technical assistance with the electron microscopy at Sheffield.

REFERENCES

1. Hankamer, B., Barber, J., and Boekema, E. J. (1997) Structure and membrane organisation of photosystem II in green plants, *Annu. Rev. Plant Physiol. Plant Mol. Biol. 48*, 641−671.
2. Horton, P., Ruban, A. V., and Walters, R. G. (1996) Regulation of light harvesting in green plants, *Annu. Rev. Plant Physiol. Plant Mol. Biol. 47*, 655−684.
3. Jansson, S. (1994) The light-harvesting chlorophyll a/b-binding proteins, *Biochim. Biophys. Acta 1184*, 1−19.
4. Jansson, S. (2000) A guide to the Lhc genes and their relatives in Arabidopsis, *Trends Plant Sci. 4*, 236−240.
5. Peter, G. F., and Thornber, J. P. (1991) Biochemical composition and organisation of higher plant photosystem II light harvesting pigment proteins, *J. Biol. Chem. 266*, 16745−16754.
6. Andersson, J., Walters, R. G., Horton, P., and Jansson, S. (2001) Antisense inhibition of the photosynthetic antenna proteins CP29 and CP26: implications for the mechanism of protective energy dissipation, *Plant Cell 13*, 1193−1204.
7. Boekema, E. J., van Breemen, J. F. L., van Roon, H., and Dekker, J. P. (2000) Conformational changes in photosystem II supercomplexes upon removal of extrinsic subunits, *Biochemistry 39*, 12907−12915.
8. Nield, J., Orlova, E. V., Morris, E. P., Gowen, B., Van Heel, M., and Barber, J. (2000) 3D map of the plant photosystem II supercomplex obtained by cryoelectron microscopy and single particle analysis, *Nat. Struct. Biol. 7*, 44−47.
9. Boekema, E. J., Hankamer, B., Bald, D., Kruip, J., Nield, J., Boonstra, A. F., Barber, J., and Rögner, M. (1995) Supramolecular structure of the photosystem II complex from green plants and cyanobacteria, *Proc. Natl. Acad. Sci. U.S.A. 92*, 175−179.
10. Boekema, E. J., van Roon, H., van Breemen, J. F. L., and Dekker, J. P. (1999) Supramolecular organization of photosystem II and its light-harvesting antenna in partially solubilized photosystem II membranes, *Eur. J. Biochem. 266*, 444−452.
11. Boekema, E. J., van Roon, H., Calkoen, F., Bassi, R., and Dekker, J. P. (1999) Multiple types of association of photosystem II and its light-harvesting antenna in partially solubilized photosystem II membranes, *Biochemistry 38*, 2233−2239.
12. Boekema, E. J., van Breemen, J. F., van Roon, H., and Dekker, J. P. (2000) Arrangement of photosystem II in crystalline macrodomains within the thylakoid membrane of green plant chloroplasts, *J. Mol. Biol. 301*, 1123−1133.
13. Yakushevska, A. E., Jensen, P. E., Keegstra, W., van Roon, H., Scheller, H. V., Boekema, E. J., and Dekker, J. P. (2001) Supramolecular organisation of photosystem II and its associated light harvesting antenna in *Arabidopsis thaliana*, *Eur. J. Biochem. 268*, 6020−6028.
14. Hankamer, B., Nield, J., Zheleva, D., Boekema, E., Jansson, S., and Barber, J. (1997) Isolation and characterization of monomeric and dimeric photosystem II complexes from spinach and their relevance to the organisation of photosystem II in vivo, *Eur. J. Biochem. 243*, 422−429.
15. Harrer, R., Bassi, R., Testi, M. G., and Schäfer, C. (1998) Nearest neighbour analysis of a photosystem II complex from Marchantia polymorpha, *Eur. J. Biochem. 255*, 196−205.
16. Zouni, A., Witt, H.-T., Kern, J., Fromme, P., Krauss, Saenger, W., and Orth, P. (2001) Crystal structure of photosystem II from Synechoccus elongatus at 3.8 Å resolution, *Nature 409*, 739−743.
17. Walters, R. G., Rogers, J. J. M., Shephard, F., and Horton, P. (1999) Acclimation of *Arabidopsis thaliana* to the light environment: the role of photoreceptors, *Planta 209*, 517−527.
18. Berthold, D. A., Babcock, G. T., and Yocum, C. F. (1981) A highly resolved, oxygen-evolving photosystem II preparation from spinach thylakoid membranes, EPR and electron transport properties, *FEBS Lett. 134*, 231−234.
19. Van Roon, H., Van Breemen, J. F. L., De Weerd, F. L., Dekker, J. P., and Boekema, E. J. (2000) Solubilization of green plant thylakoid membranes with n-dodecyl-,D-maltoside. Implications for the structural organization of the photosystem II, photosystem I ATP synthase and cytochrome b 6/f complexes, *Photosynth. Res. 64*, 155−166.
20. Ruban, A. V., Young, A., Pascal A., and Horton, P. (1994) The effects of illumination on the xanthophyll composition of the photosystem II light harvesting complexes of spinach thylakoid membranes, *Plant Physiol. 104*, 227−234.
21. Ruban, A. V., Lee, P. J. Wentworth, M., Young, A. J., and Horton, P. (1999) Determination of the stoichiometry and strength of binding of xanthophylls to the photosystem II light harvesting complexes, *J. Biol. Chem. 274*, 10458−10465.
22. Van Heel, M., and Frank, J. (1981) Use of multivariate statistics in analysing the images of biological macromolecules, *Ultramicroscopy 6*, 187−194.
23. Van Heel, M. (1989) Classification of very large electron microscopical image data sets, *Optik 82*, 114−126.
24. Rigoni, F., Barbato, R., Friso, G., and Giacometti, G. M. (1992) Evidence for direct interaction between chlorophyll proteins CP29 and CP47 in photosystem II, *Biochem. Biophys. Res. Comm. 184*, 1094−1100.
25. Bassi, R., and Dainese, P. (1992) A supramolecular light harvesting complex from chloroplast photosystem II membranes, *Eur. J. Biochem. 204*, 317−326.

BI027109Z